



Supplementary Materials for

Competition between engrams influences fear memory formation and recall

Asim J. Rashid, Chen Yan, Valentina Mercaldo, Hwa-Lin (Liz) Hsiang, Sungmo Park, Christina J. Cole, Antonietta De Cristofaro, Julia Yu, Charu Ramakrishnan, Soo Yeun Lee, Karl Deisseroth, Paul W. Frankland,* Sheena A. Josselyn*

*Corresponding author. Email: sheena.josselyn@sickkids.ca (S.A.J.); paul.frankland@sickkids.ca (P.W.F.)

Published 22 July 2016, *Science* **353**, 383 (2016)
DOI: 10.1126/science.aaf0594

This PDF file includes:

Materials and Methods
Supplementary Text
Figs. S1 to S9
Tables S1 to S7
References

Materials and Methods

Mice

Adult (at least 10 weeks of age) male and female F1 hybrid (C57BL/6NTac x 129S6/SvEvTac) wild-type (WT) mice were used for all experiments, except where noted. Mice were bred at the Hospital for Sick Children and group housed (4 per cage) on a 12 h light/dark cycle with food and water available *ad libitum*. Behavioral experiments took place during the light-phase. All procedures were conducted in accordance with policies of the Hospital for Sick Children Animal Care and Use Committee and conformed to both Canadian Council on Animal Care (CCAC) and National Institutes of Health (NIH) Guidelines on Care and Use of Laboratory Animals.

PV-Cre knockin driver transgenic mice (B6;129P2-*Pvalb*^{tm1(cre)Arbr/J}) which express Cre recombinase in PV neurons, without disrupting endogenous PV expression, were originally generated by Silvia Arber, FMI (26), and obtained from Jackson Lab. Heterozygous PV-Cre mice were maintained on a C57BL/6 genetic background.

Fear conditioning

The same general procedure was used for fear conditioning (training). Mice were placed in a conditioning chamber (*Context A*) and allowed to habituate for 2 min before presentation of a 30-sec auditory CS that terminated with a 2-sec footshock. Mice remained in chamber for an additional 30 sec before being returned to home-cage. A similar procedure was used for memory testing. 24 h after the last training event, mice were placed in a novel context (distinct from conditioning chamber) and, after 2 min, presented with CS for 1 min. Memory was assessed by measuring percent time spent freezing (cessation of all movement except respiration) during CS presentation via automated procedures (7) or hand-scoring of videos (average of two scorers unaware of the treatment conditions in optogenetic experiments).

For the sake of clarity, we did not present baseline (pre-CS) freezing scores for these experiments. Mice generally showed low freezing when placed in a novel context and that there was no difference between groups in this baseline freezing.

The specific behavioral procedures for each experiment are as follows:

Discrimination between auditory CS1 and CS2 in fear conditioning experiments (Fig. 1A)

To test whether mice were able to distinguish between two auditory conditioned stimuli (CSs) in fear conditioning experiments, we used two auditory CSs [CS1 (auditory pips, 1.9 Hz pulses of auditory pips, 2-ms rise and fall, 7500 Hz, 85 dB, 30 sec), CS2 (auditory tone, 2800 Hz, 85 dB, 30 sec), counterbalanced]. Mice were fear conditioned to CS1 (or CS2, counterbalanced) by pairing CS1 with a footshock (0.45mA, 2s that co-terminated with the CS) in *Context A*. 24 h later, mice were placed in a novel context (*Context B*) and 2 min later, presented with the second untrained CS for 1 min (e.g. CS1-US training, CS2 testing). 24 h later mice were similarly tested for the trained CS (e.g. CS1-US training, CS1 testing) in *Context C* (see Table 1 below). The order of testing for CS1 and CS2 were counterbalanced across mice. As there were no order effects in CS testing, groups were averaged. **Fig. 1A** shows mice readily discriminate between CSs, freezing significantly more to the trained CS and we observed no difference between levels of freezing to the trained CSs. A *Training Condition* (CS1-shock, CS2-shock) X

Test Condition (CS1, CS2) ANOVA showed a significant interaction, $F(1,12) = 44.29$, $P < .001$. Post-hoc Newman-Keuls tests on the significant interaction revealed that mice froze significantly more to the trained CS than non-trained CS and that the levels of freezing to the trained CS did not differ, indicating equal associability of each CS.

Table 1: Experimental design for Fig. 1A

<i>Group</i>	<i>Test1</i>	<i>Test2</i>
CS1+shock (0.45mA)	CS2*	CS1
CS2+shock (0.45mA)	CS1	CS2

*order of testing counterbalanced

Two Events separated by different intervals (Fig. 1B)

Mice were exposed to two events (Event1, Event2) separated by different inter-trial intervals. For all groups, Event2 was identical and consisted of placing mice in *Context B* and, 2 min later pairing CS2 with footshock (0.45mA, 2 sec). The content and timing of Event1 differed between three groups.

1. Prior learning group (filled orange bars in **Fig. 1B**). Event1 consisted of CS1+footshock training. Mice were placed in *Context A* and, 2 min later, CS1 was paired with footshock (0.4mA, 2 sec). Mice remained in chamber for an additional 30 sec before being returned to home-cage. Event1 occurred either 1.5, 3, 6, 18 or 24 h before Event2 (CS2+footshock training).
2. Prior CS1 (tone) alone group (CS1 alone, open purple bar). Event1 consisted of CS1 alone exposure (without footshock). Mice were placed in *Context A* and, 2 min later, CS1 alone was presented. Mice remained in chamber for an additional 30 sec before being returned to home-cage. Event1 occurred either 1.5, 3, 6, 18 or 24 h before Event2 (CS2+footshock training). This group was designed to control for the effects of prior exposure to CS1. Data were averaged into a single prior CS1 alone control group and presented in **Fig. 1B**. The freezing scores for each time-point group are presented in **fig. S1A**.
3. Prior immediate shock alone group (Imm shock, open gray bar). Event1 consisted of placing mice in *Context A* followed by immediately by a footshock (0.4mA, 2 sec) either 6 h or 24 h prior to Event2 (CS2+shock training). An additional group received a stronger immediate footshock (0.8mA, 2 sec) 6 h prior to Event 2. Importantly, previous research shows that training with an immediate footshock does not induce learning (27-29). These immediate shock groups designed to control for potential sensitization effects of prior footshock.

Supplementary Figure 1

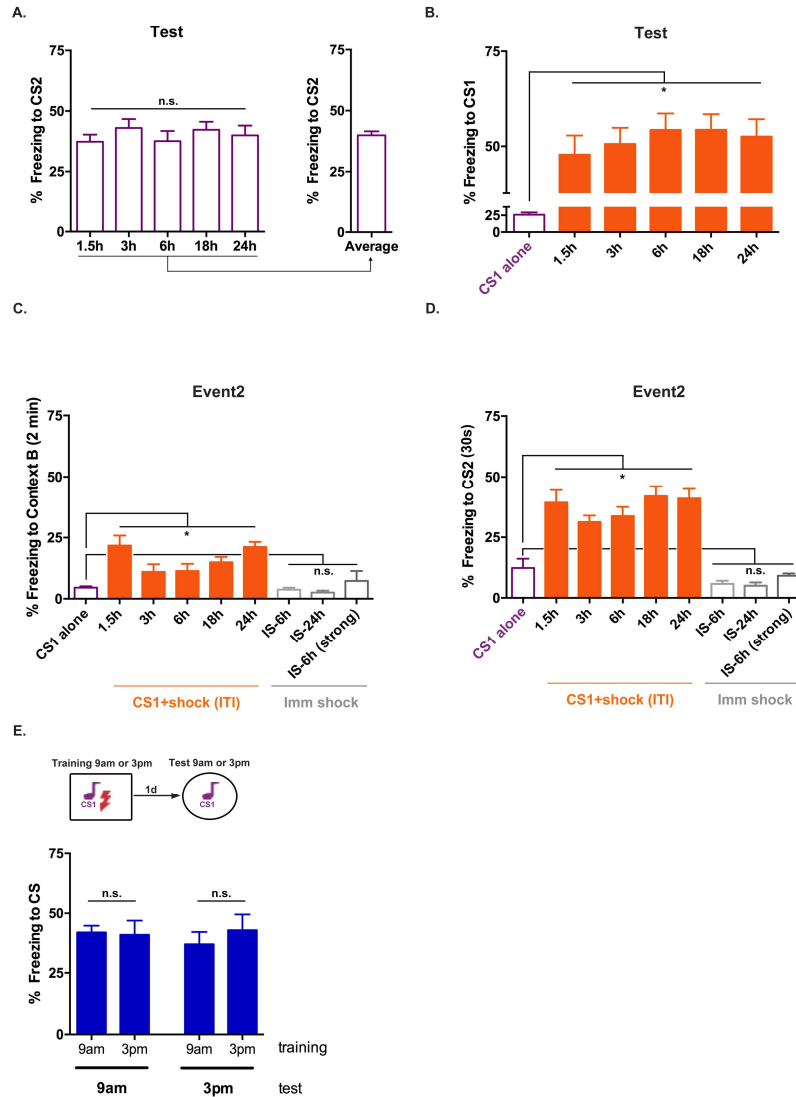


Fig. S1. Analysis of behavior during two-memory experiments

- A. CS1 alone groups (Event2 memory).** Fig. 1B presented freezing scores for CS2 during the test as an average of all CS1 alone groups (open purple bar). This group is comprised of 5 groups that received CS1 alone (for Event1) either 1.5, 3, 6, 18 or 24 h prior to Event2 (to match the timing of different ITIs in the experimental groups). There was no difference between CS1 alone groups in terms of freezing during Event2 memory test, $F(4,51) = 0.91, P > .05$. Therefore, we averaged these groups (presented in *Right* graph, Fig. 1B). $n=12, 12, 12, 8, 12$ for each group, 56 for average.
- B. Memory for Event1 is not affected by timing of subsequent Event2 training.** No effect of ITI between Event1 and Event2 on memory for Event1. During Event2 all groups were given CS2+shock. Mice exposed to CS1 without shock (CS1 alone group) for Event1 showed low levels of freezing but all ITI groups (1.5-24h between Event1 [CS1+shock] and Event2 [CS2+shock]) showed similar levels, $F(5,118) = 23.34, P < .001, n=56, 12, 16, 16, 12, 12$ per group, respectively.
- C. Freezing during Event2 training (Context B initial freezing levels).** Freezing to Context B (2 min prior to CS2 presentation) during Event2 training for all groups presented in Fig. 1B. Previously trained groups (CS1+shock for Event1), showed higher freezing than CS1 alone or immediate shock groups, $F(8,142) = 11.31, P < .001$. Importantly, there was no difference in freezing between CS1+shock groups (closed orange bars) trained with different ITIs, $F(4,51) = 0.91, P > .05, n=56, 12, 16, 16, 12, 12, 10, 12, 5$ per group, respectively.
- D. Freezing during Event2 training (CS2 freezing levels).** Freezing to the 30-sec presentation of CS2 during Event2 training for groups in Fig. 1B. Previously trained groups (CS1+shock for Event1), showed higher freezing than CS1 alone or immediate shock groups, $F(8,142) = 30.49, P < .001$. However, there was no difference in freezing between CS1+shock groups (closed orange bars) trained with different ITIs, $F(4,51) = 0.91, P > .05, n=56, 12, 16, 16, 12, 12, 10, 12, 5$ per group, respectively.
- E. Control for time-of-day effects on fear conditioning.** Mice were trained once at 9am or 3pm (CS1+ footshock, 0.45 mA) and tested the following day at 9am or 3pm. There was no difference in freezing levels between groups [$F(3,27) = 0.22, P > .05$] indicating that under the present training conditions, time-of-day effects do not significantly contribute to the observed effects. $n=8$ per group.

Freezing scores for all groups during CS2 presentation in Event2 (training), are shown in **fig. S1D**. In all groups, memory test for Event2 (or Event1, counterbalanced) occurred the day after Event2. Mice were placed in *Context C* and CS2 replayed for 1 min. 24 h later, memory for Event1 was tested. Mice were placed in *Context D* and CS1 replayed for 1 min (see *Tables 2 and 3 below*). Freezing scores for Event2 memory are shown in **Fig. 1B** while scores for Event1 memory are shown in **fig. S1B**.

Table 2: Experimental design for Fig. 1B

<i>Event1</i>	<i>Event2</i>	<i>Inter-training interval</i>
CS1+shock (0.4mA)	CS2+shock (0.45mA)	1.5, 3, 6, 18 or 24 h
CS1 alone	CS2+shock (0.45mA)	1.5, 3, 6, 18 or 24 h (no difference between groups on subsequent CS2 freezing, so averaged into single control group)
Immediate shock (Imm shock) alone (0.4mA, 0.8mA)	CS2+shock (0.45mA)	6 or 24h

Training and testing contexts were as follows:

Table 3: Design of different contexts

<i>Context</i>	<i>Dimensions</i>	<i>Floors</i>	<i>Walls</i>	<i>Lighting (relative to maximum brightness)</i>	<i>Scent</i>
A	rectangle 714 cm ²	2.5mm diam dark gray bars	dull silver walls, white sheet over door	50%	water
B	rectangle 700 cm ²	1.5mm diam chrome-colored bars	silver walls, door uncovered	30%	mint
C	triangle 357 cm ²	smooth white plastic	black walls, door uncovered	40%	vanilla
D	semi-circle 275.2 cm ²	rough white plastic	white plastic, door covered with sheet of white/black bars	10%	ethanol

Two Events separated by different intervals using CSs of different modalities (fig. S2A)

To control for potential generalization between the two auditory CSs used in the above experiments, we conducted an additional experiment that used a light CS for Event1 and an auditory CS for Event2. Mice were first trained on Event1 [overhead light, luminous emittance of 500-600 lux, for 30 sec co-terminating with footshock, 0.4mA, 2 sec) and trained on Event2 (auditory stimulus CS2 co-terminating with footshock, 0.45mA, 2 sec). Event1 occurred either 6 or 24h prior to Event2. A control group receive light alone presentation 6h prior to Event2.

Two Event FISH experiments to visualize engram overlap (Fig. 1C)

To visualize neurons activated by memory retrieval induced by re-exposure to CS1 and CS2 in the two-memory experiments (as a proxy for the engram underlying each memory), we trained and tested four groups of mice (*summarized in Table 4 below*).

1. CS1-CS1 Group. Mice were trained for Event1 only [CS1+footshock (0.4mA)]. 24h later, mice were tested for CS1 (placed in *Context C* and 2 min later presented with CS1 for 3 min). Neurons activated by this exposure were identified as *h1a*⁺. Mice were then placed in a quiet holding room for 25 min, followed by placement in *Context D* and 2 min later, presented with CS1 again for 3 min. Neurons activated by this exposure were identified as *arc*⁺. 5 min later, brains were quickly removed and frozen. In this group, mice were trained for one event only (CS1+footshock) and tested twice for the same event memory. This control group was included to determine the percentage overlap of LA neurons activated by testing the same memory twice (as a means of assessing the upper-limit “ceiling” of overlap).
2. CS1-CS3 Group. Mice were trained for Event1 only [CS1+footshock (0.4 mA)]. 24h later, mice were tested for CS1 (placed in *Context C* and 2 min later presented with CS1 for 3 min). Mice were then placed in a quiet holding room for 25 min, followed by placement in *Context D* and 2 min later, presented with a novel CS (CS3) again for 3 min. Half of the mice were tested for CS3 and CS1 in reverse order (no difference was observed between order presentations). In this group, mice were trained for one event only and tested for this learned CS and a novel CS. This control group was included to determine the percentage overlap of LA neurons activated by testing a memory and a novel CS (as a means of assessing the lower-limit “floor” of overlap).
3. CS1-CS2 (6h interval) Group. Mice were trained on two events [CS1+footshock (0.4 mA), CS2+footshock (0.45 mA)] with a 6h inter-training interval. 24h following Event2 (CS2+shock), mice were placed in *Context C*, and 2 min later presented with CS2 for 3 min. Mice were then placed in a quiet holding room for 25 min, followed by placement in *Context D* and 2 min later, presented with CS1 for 3 min.
4. CS1-CS2 (24h interval) Group. Mice were trained on two events as above [CS1+footshock (0.4 mA), CS2+footshock (0.45 mA)], but with a 24h inter-training interval. Testing was conducted as above.

Supplementary Figure 2

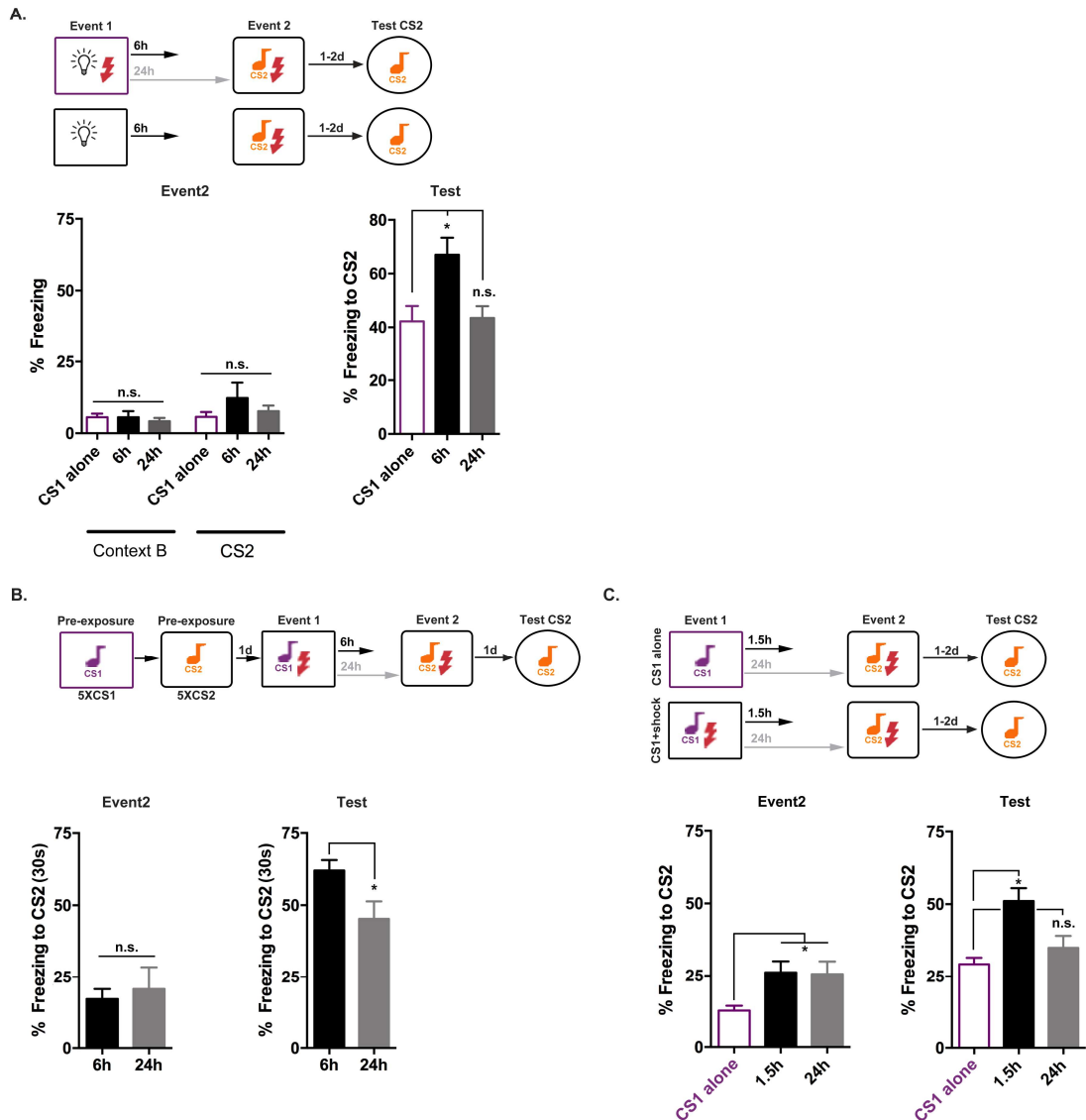


Fig. S2. Examining generalization between CSs in two-memory experiments

- A. Using CSs of different modalities.** Mice were trained with Event1 (light-shock pairing) followed either 6h or 24h by Event2 (auditory stimulus-shock training). During Event2 training, both groups of mice showed similarly low levels of freezing when initially placed in Event2 training context, $F(2,21) = 0.27, P > .05$ and low levels of CS2-freezing, $F(2,21) = 0.96, P > .05$. However, when tested for Memory2, mice with short ITI (6h) showed significantly greater freezing than mice trained with longer ITI (24h), similar to the effects observed in Fig. 1B using two auditory CSs, $F(2,21) = 6.33, P < .001, n=8$ per group.
- B. Pre-exposure to two auditory CSs to reduce generalization.** Mice were pre-exposed to CS1 (5 x 1 min) and CS2 (5 x 1 min). The following day, mice were trained with Event1 followed either 6h or 24h by Event2 (exactly as in Fig. 1B). During Event2 training, both groups of mice showed similarly low levels of CS2-freezing, $F(1,14) = 0.16, P > .05$. However, when tested for Memory2, mice with short ITI (6h) showed greater freezing than mice trained with longer ITI (24h). Using this protocol, generalization to CS2 during Event2 was reduced in both 6h and 24h groups (*left graph*, compare to fig. S1D), but memory enhancement in the 6h but not 24h group was still observed during Event2 memory test (*right graph*), $F(1,14) = 5.56, P < .001, n=8$ per group.
- C. Weak training conditions to reduce generalization between auditory CSs.** Mice were trained in Event1 and Event2 (no CS pre-exposure) using footshocks of weak intensity (0.25mA for Event1, 0.3mA for Event2), or exposed to CS1 alone 1.5h or 24h before Event2 (averaged into CS1 alone group). During Event2, all groups showed low levels of freezing during CS2 presentation (*left graph*, compare to fig. S1D), with CS1 alone mice freezing less. Mice trained with short ITI froze more in Event2 memory test than similarly trained mice with longer ITI or mice that received CS1 alone $F(2,45) = 11.27, P < .001$, similar to the effect observed in Fig. 1B. $n=24, 12, 12$.

Table 4: Experimental design for Fig. 1C

<i>Group</i>	<i>Training</i>	<i>Interval</i>	<i>Test1 (h1a)</i>	<i>Test2 (arc)</i>
CS1-CS1	CS1+shock (0.4mA) only	n/a	CS1	CS1
CS1-CS3	CS1+shock (0.4 mA) only	n/a	CS1	CS3
CS1-CS2 (6h)	CS1+shock (0.4mA), CS2+shock (0.45 mA)	6h	CS1	CS2
CS1-CS2 (24h)	CS1+shock (0.4mA), CS2+shock (0.45 mA)	24h	CS1	CS2

Freezing scores for these groups are presented in **fig. S3A** (first min of each 3-min test).

For FISH analyses, tissue was sectioned (20 μ m) and prepared for FISH as previously described. *arc* mRNA expression was visualized using a DIG-conjugated anti-sense probe corresponding to the full length open reading frame of *arc* (7, 8). For *homer 1a (h1a)*, an FITC-conjugated anti-sense probe corresponding to nucleotides 4457-4915 (exon 5') was used (30). Sections from 4 mice were mounted on the same slide to minimize differences in staining and visualization conditions. After hybridization and amplification of *arc* and *h1a* signals, sections were counterstained with Hoechst 33258 to visualize nuclei.

Sections were imaged on a laser confocal microscope (Zeiss LSM 710). For each image, an optical z-stack series was acquired with images $\leq 1 \mu$ m apart. Stacks were analyzed for nuclear *arc* and nuclear *h1a* by two individuals unaware of treatment condition. At least four sections were counted for each mouse, and counts were averaged such that each mouse had one score. The proportion of neurons activated during recall of Event1 was calculated as $pArc_{nuc}$ (nuclear *arc* signal/total nuclei), for Event2 $pH1a$ (nuclear *h1a* signal/total nuclei). The probability of memory co-allocation was calculated as $parc/h1a$ ($(arc+h1a \text{ co-label})/[h1a + arc] - [h1a+arc \text{ co-label}]$).

The overlap of LA engrams was further examined with additional intervals between Event1 and Event2 using nuclear localized versus cytoplasmic localized *arc* mRNA as a marker of recent versus more remote neuronal activity (**fig. S3B**). The proportion of neurons activated during recall of Event1 was calculated as $pArc_{nuc}$ (nuclear *arc* signal/total nuclei), for Event2 $pArc_{cyt}$ (cytoplasmic *arc* signal/total nuclei). The probability of memory co-allocation was calculated as $parc_{dble}$ (nuclear and cytosolic co-label/[nuclear *arc* + cytoplasmic *arc*] - [nuclear and cytosolic co-label]). For cases where it was difficult to distinguish between nuclear and/or cytoplasmic *arc* signal, those neurons were excluded from the analysis (approx. 1% of neurons in each condition).

Supplementary Figure 3

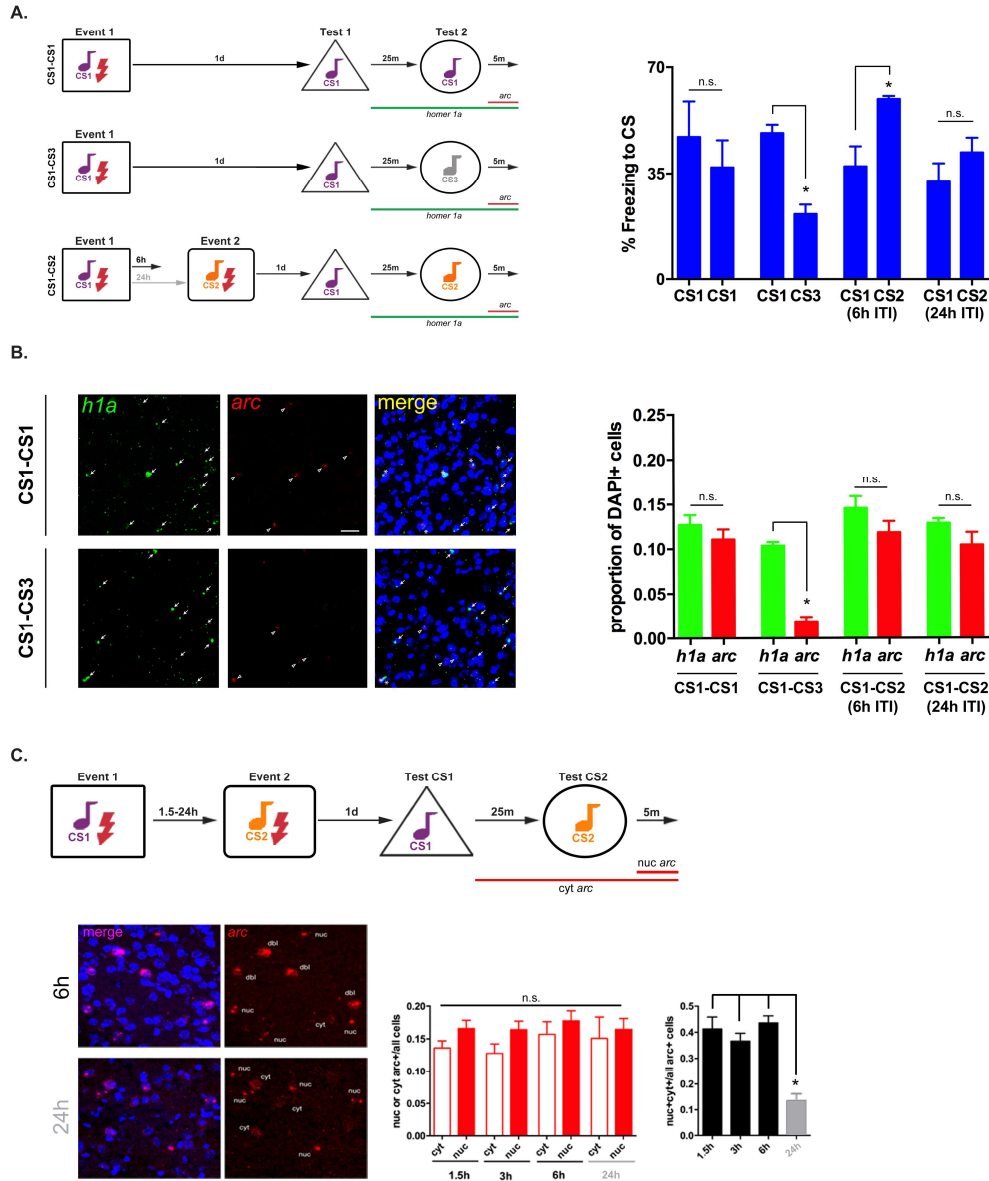


Fig. S3. FISH analysis of the overlap of engrams supporting memories for two events with different inter-training intervals (ITIs)

- A.** *Left.* Experimental time-line. *Right.* Freezing data for FISH experiments depicted in Fig. 1C. Overall CS freezing levels were similar, except freezing to the novel CS (CS3) was lower than to trained CSs and mice trained with a 6h ITI showed higher freezing to CS2. Group [CS1-CS1, CS1-CS3, CS1-CS2 (6h ITI), CS1-CS2 (24h ITI)] X Test (CSs) ANOVA showed a significant interaction, $F(3,8) = 15.3, P < .001$. $n=3$ mice/group.
- B.** *Left.* Examples of *h1a* and *arc* staining for control groups (CS1-CS1, CS1-CS3). Cells expressing mRNA for *h1a* (green signal, solid arrows, Event1), *arc* (red signal, open arrows, Event2) and both *h1a* and nuclear *arc* (asterisks). Scale bar = 20 μ m. *Left.* Overall percent *arc*⁺, *h1a*⁺ neurons did not differ between groups, except that exposure to a novel CS induced less of the activity marker (*arc*). Group [CS1-CS1, CS1-CS3, CS1-CS2 (6h ITI), CS1-CS2 (24h ITI)] X Activity marker (*h1a*, *arc*) ANOVA showed a significant interaction, $F(3,8) = 42.58, P < .001$. This shows that both markers label active cells to similar extent and that the size of the LA engram was stable. $n=3$ mice/group
- C.** In addition to *h1a* and *arc* co-staining to determine engram overlap, we also used nuclear (nuc) and cytoplasmic (cyt) *arc* signal. *Top.* Time-line of experiment. *Left.* Images with and without Hoechst 33258 signal (blue) for 6h ITI and 24h ITI groups. *Right.* As with *h1a/arc* analysis, all groups showed equivalent proportions of cytoplasmic and nuclear *arc*⁺ neurons, indicating that the overall size of the LA component of the engram was stable [no effect of ITI on overall level of nuc *arc* $F(3,10) = 0.22, P > .05$ or cyto *arc* $F(3,10) = 0.48, P > .05$]. *Far right.* Nearly 3-fold increase in overlap of nuc and cyt *arc* signal in groups trained with short ITI (1.5, 3 or 6h) when compared to longer ITI (24h), $F(3,10) = 16.51, P < .001$. $n=3$ or 4 mice per group, 4 sections analyzed per mouse.

Extinction experiment to examine whether memories are functionally linked (Fig. 1D)

To examine whether the memory for events trained with a short (6h) inter-training interval are functionally linked, we examined whether experimentally extinguishing Memory2 would impact Memory1. Three groups of mice were included in this experiment (see Table 5 below). Groups 1 and 2 were trained on Event1 [CS1+footshock (0.4 mA)] and Event2 [CS2+footshock (0.45 mA)], with 6h or 24h inter-trial intervals. Group3, a control group, was trained on Event1 only [CS1+footshock (0.4 mA), similar to Groups 1 and 2], and 6h following Event1, was exposed to CS2 alone (in the absence of footshock). The next day, all groups were tested for CS1 (*Context C*, 1 min presentation of CS1). 24h later, mice were placed in *Context D* and CS2 was presented alone (without footshock) five times for 1 min, separated by 1 min (CS2 extinction training). The first exposure to CS2 was used to gauge pre CS2-extinction freezing (closed bars in Fig. 1D). Importantly, CS1 was not presented during this extinction training and was never explicitly extinguished. The day following extinction training, memory for each event was tested by presenting CS1 and CS2 alone (open bars, post-CS2-extinction freezing levels), as above. Mice in Group 3 were included to control for the effect of multiple CS2 presentations on freezing to CS1.

Table 5: Experimental design for Fig. 1D

<i>Group</i>	<i>Training</i>	<i>Interval</i>	<i>Extinction</i>
Group1, CS1-CS2 (6h)	CS1+shock (0.4mA), CS2+shock (0.45mA)	6h	CS2
Group2, CS1-CS2 (24h)	CS1+shock (0.4mA), CS2+shock (0.45mA)	24h	CS2
Group3, CS1+shock control	CS1+shock (0.4mA), CS2 alone	6h	CS2

The effects of recall on subsequent memory for a second event experiment (Fig. 4D)

This experiment examined whether recall of a previously acquired Event1 memory shortly before Event2 would impact memory for Event2. There were 3 groups. All groups were trained on Event1 (CS1+footshock, 0.4mA). 24h later two groups were re-exposed to CS1 in *Context B* (for 1 min). Either 6h (Group1) or 24h (Group2) later, mice were trained for Event2 (CS2+shock, 0.45mA). A control group (Group3) was trained for Event1 as above, but not re-exposed to the CS1 again. This group was simply placed in the novel context for the same length of time as Groups1 and 2 and was designed as a “no recall” control. All groups were tested for Event2 (CS2 freezing) 24h later (see Table 6 below).

Table 6: Experimental design for Fig. 4D

<i>Group</i>	<i>Event1</i>	<i>Recall</i>	<i>Time between recall of CS1 and Event2</i>	<i>Event2</i>
1 Recall 6h	CS1+shock(0.4mA)	CS1	6h	CS2+shock(0.45mA)
2 Recall 24h	CS1+shock(0.4mA)	CS1	24h	CS2+shock(0.45mA)
3 No recall	CS1+shock(0.4mA)	No recall	No CS1 recall, only context, 6h	CS2+shock(0.45mA)

In vivo pCREB analysis following fear conditioning (Fig. 2A)

WT mice were randomly divided into the following treatment groups; 1) fear conditioning + 1.5h, 2) fear conditioning + 6h, 3) fear conditioning + 18h, 4) fear conditioning + 24h, 5) homecage, 6) CS alone+6h, and, 7) immediate shock alone+6h. Mice were fear conditioned [single CS+footshock (0.45mA)] or received either the tone CS alone or immediate footshock (0.45mA) alone and returned to homecage. Mice were perfused either 1.5, 6, 18 or 24h later. Homecage mice were taken directly from homecage and not exposed to conditioning chamber, auditory CS or footshock. Therefore, there were three control groups in this experiment (homecage, CS alone 6h prior to perfusion, immediate shock alone 6h prior to perfusion).

Immunostaining for pCREB and total CREB was performed as previously described (31) on 12-16 sections per mouse, spanning the antero-posterior axis of the LA. Sections were processed and imaged in parallel under identical conditions. Briefly, sections were incubated with rabbit anti-pCREB polyclonal antibody (1:3000, Millipore cat#06519) overnight at 4°C, followed by a 2 h incubation at room temperature with a biotinylated goat anti-rabbit secondary antibody (111-065-144; 1:1 000, Jackson ImmunoResearch, West Grove, PA). Staining was visualized using avidin-biotin peroxidase coupled to diaminobenzidine. Before mounting, sections were lightly counterstained with 1% Neutral red. The LA was imaged (with a 10X objective) and number of pCREB⁺ nuclei quantified using Image J software (NIH) (31). Basal staining was determined by averaging pCREB signal intensity in sections from homecage mice and pCREB⁺ cells in all conditions were identified as signal if 2 standard deviation units above the mean. Parallel sections from same mice were immunostained for total CREB using a rabbit anti-CREB polyclonal antibody (9197, 1:1000, Cell Signaling). No differences in total CREB levels were noted between groups.

Supplementary Figure 4

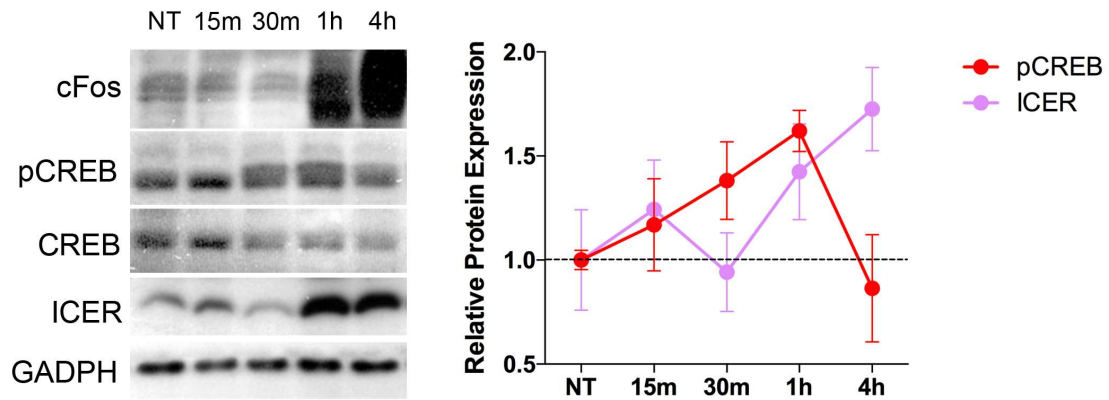


Fig. S4. Neuronal stimulation transiently increases activated CREB followed by an increase in inhibitory CREB isoform, ICER

KCl/forskolin stimulation of primary hippocampal neurons produced a transient increase in pCREB compared to non-treated cells (NT) that peaks 1 h after stimulation and returns to baseline by 4 h. This stimulation also increases expression of the inhibitory CREB isoform ICER [inducible cyclic adenosine monophosphate (cAMP) early repressor] that peaked at 4h. Total CREB levels not changed by stimulation.

Right, western blot, with GADPH as loading control.

Left, quantification of results, $F(4,15) = 5.67$, $P < 0.05$. $n=8$ for each time point.

Viral vectors

Herpes virus (HSV)-based amplicons

We chose to use HSV vectors to manipulate excitability in LA principal neurons because HSV is naturally neurotropic (32). Following microinjection into the LA, HSV infects roughly 10-20% of principal neurons, rather than glia or inhibitory neurons. In agreement with previous findings (10, 33) HSV infects primarily principal excitatory neurons in the LA (see **fig. S6**).

Transgene expression using this viral system typically peaks 3 d, and dissipates within 10-14 d, following microinjection (34). 3-7 d following microinjection into LA, we observed no evidence of retrograde transport using this vector (8). HSV virus was packaged using a replication-defective helper virus, purified on a sucrose gradient, pelleted and resuspended in 10% sucrose, as previously described (30, 31). The average titer of the virus stocks was 4.0×10^7 infectious units/ml.

The following HSV-derived amplicons were synthesized and used in behavioral experiments:

HSV-NpACY: containing enhanced channelrhodopsin2 (ChR2-H134R) fused to enhanced yellow fluorescent protein (eYFP) and halorhodopsin 3.0 (NpHR3.0) to enable bidirectional control of neuronal activity (see **Fig. 3A**). These two opsins are spectrally compatible; neurons can be excited by blue light (473 nm) activation of ChR2 and inhibited by red light (660 nm) activation of NpHR3.0. Using red light, rather than yellow, efficiently activates NpHR3.0 while minimizing cross-talk with ChR2 (17, 18). Opsin genes were connected in the viral vector using a 2A self-cleavage linker derived from porcine teschovirus (P2A) and expression was driven by the endogenous HSV promoter IE4/5. We characterized this vector both using both *in vitro* and *in vivo* assays (see **figs. S5, S7A**).

HSV-vCREB: containing wild-type full-length CREB fused to green fluorescent protein (GFP) (kindly provided by Dr. Satoshi Kida, Tokyo University of Agriculture, Tokyo, Japan) with expression driven by the IE4/5 promoter.

HSV-vCREB/hM4Di: similar to HSV-vCREB above, but with inhibitory DREADD hM4Di (kindly provided by Dr. Bryan Roth, UNC) inserted after a downstream CMV promoter. Control amplicons were HSV expressing GFP or hM4Di (after IE4/5 or CMV promoters, respectively).

Adeno-associated virus (AAV)

AAV8-hSyn-DIO-hM4Di-mCherry was obtained from UNC Vector Core (Chapel Hill, NC). In this viral vector, the double floxed inverse open reading frame of hM4Di fused to mCherry can be expressed from the human synapsin (hSyn) promoter after Cre-mediated recombination (35). These AAV viruses were microinjected into the amygdala of PV-Cre mice, enabling specific expression of hM4Di in parvalbumin-expressing interneurons (PV⁺ cells). Further manipulations and behavioral experiments were performed on these mice 4 weeks after AAV-infusion. We verified this construct in **fig. S7C**.

Supplementary Figure 5

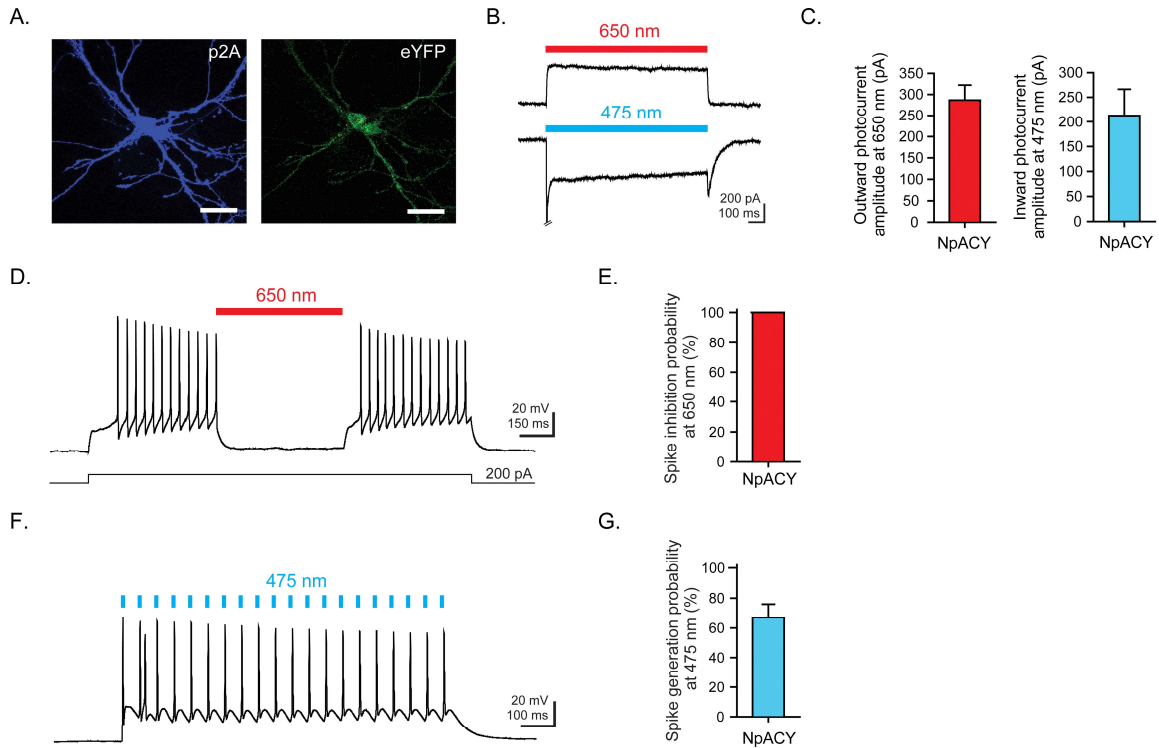


Fig. S5. Characterization of NpACY construct

- Confocal image of NpACY-expressing neurons with both p2A immunostaining and eYFP fluorescence. Scale bar = 40 μm .
- Representative voltage-clamp traces from an NpACY-expressing neuron after blue (475/28 nm, top trace) and red (650/13 nm, bottom trace) light application. Escape spike within peak current during blue light is truncated for clarity.
- Bar graph summary of photocurrent amplitudes after blue and red light delivery.
- Sample current-clamp trace showing red light-mediated inhibition of electrically-induced spiking in an NpACY-expressing neuron (200 pA electrical current injection).
- Bar graph summary of spike inhibition probability under red light.
- Sample current-clamp trace showing blue light-induced action potentials in the same neuron. Blue light pulse widths were 5 ms, delivered at 20 Hz.
- Spike generation probability under blue light. Light power density: 6.3 mW/mm² for red light, 10.3 mW/mm² for blue light. $n=13$ cells.

Supplementary Figure 6

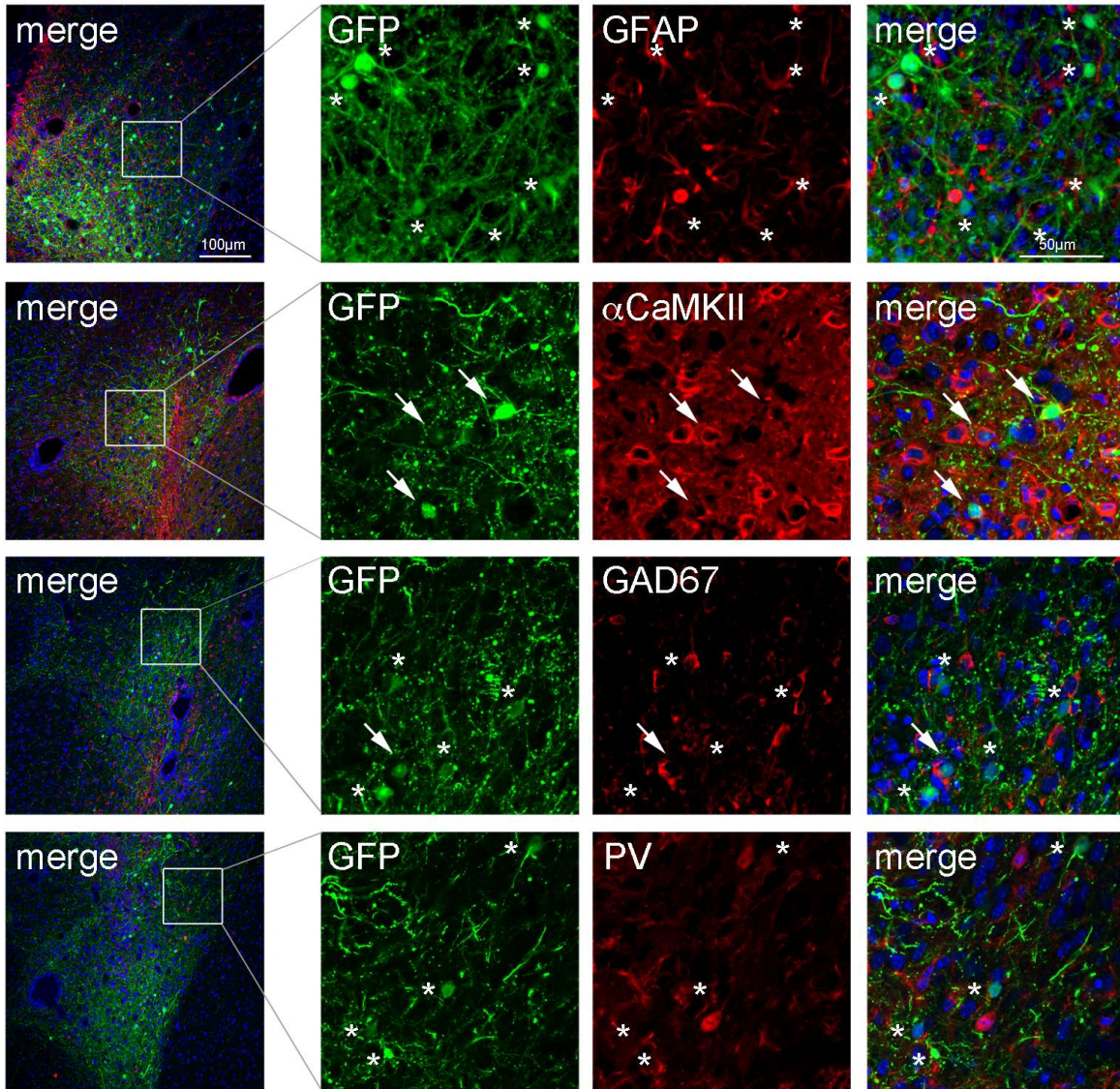


Fig.S6 Characterization of HSV infection

Following microinjection into LA, HSV vectors overwhelmingly infect excitatory principal neurons (α CaMKII⁺) (~ 99%). Mice were microinjected with HSV expressing GFP into the LA, and 4 days later infected cells were phenotyped using immunohistochemistry for various cell markers.

DAPI (blue, nuclear stain), GFP (green, infected cell), various cell markers (red).

We observed no (0%) HSV-infected cell that co-expressed endogenous markers typical of astrocytes (GFAP, glial fibrillary acidic protein, depicted as *) and all infected cells were positive for α CaMKII as a marker of excitatory pyramidal/principal neurons (arrows). There was no overlap between GFP and PV (parvalbumin) neurons. Only very rarely (~ 1%) did HSV-infected cells co-express GAD67 (Glutamate decarboxylase 67), a marker of an inhibitory neuron.

Supplementary Figure 7

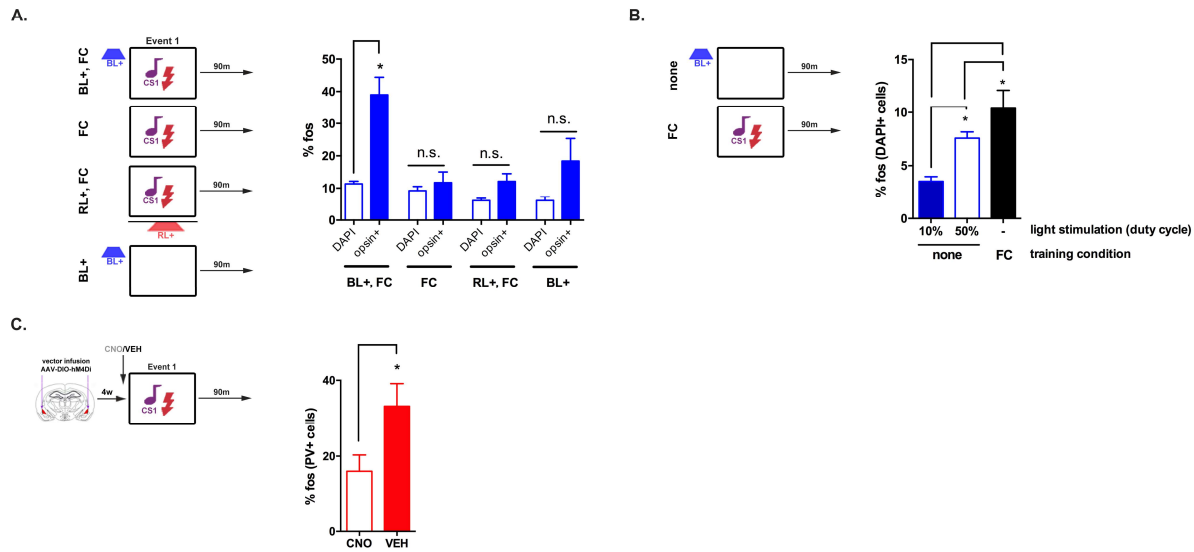


Fig. S7 Validation of constructs

- A. To verify that blue light (BL+) increased activity of HSV-NpACY expressing neurons, mice were microinjected with NpACY vector and LA cfos was analyzed following several treatments (depicted in experimental time-line, *Right*). Percent LA cfos was compared in a *Neuron* (infected vs. non-infected) X *Treatment* (NpACY, fear conditioning, BL+ vs. NpACY, fear conditioning, BL- vs. NpACY, fear conditioning, RL+ vs. NpACY, BL+) ANOVA, which revealed a significant interaction, $F(3, 55) = 4.19, P < .001$. Post-hoc Newman-Keuls comparisons showed that ¹ neurons infected with NpACY had greater cfos than non-infected neighbors if these neurons were excited with blue light before training (BL+, FC), ² there is no increase in cfos in neurons infected with NpACY relative to their non-infected neighbors if these neurons were NOT excited before training (BL-, FC), nor was there an increase in cfos in neurons infected with NpACY relative to their non-infected neighbors if these neurons were inhibited during training (RL+, FC), and, ³ neurons infected with NpACY show slightly (but not statically significant) higher cfos than their non-infected neighbors if these neurons were excited even in the absence of training (BL+, no FC). These findings validate the use of these constructs. $n=9-21$ sections/group.
- B. Examining the potential effects of blue light alone on cellular activity. Mice were microinjected with HSV-GFP (no opsin) vector and shone blue light at 10% duty cycle (as in our behavioral experiments) and 50% duty cycle, and LA cfos levels were compared to mice that were fear conditioned but did not receive light. An ANOVA revealed a significant effect of *Treatment*, $F(2,82) = 16.99, P < .001$. Post-hoc comparisons showed that mice with 50% duty cycle showed higher cfos than 10% duty cycle, but less than mice that were fear conditioned. The levels of cfos in mice that received 10% duty cycle (the training conditions in most of our experiments in the present manuscript) were very low (3.5%) and comparable to homecage levels. $n=31$ and 36 sections for 10% and 50% duty cycles, respectively, $n=18$ for FC group.
- C. To validate the DREADD construct (hM4Di) used in **Fig. 4** and **fig. S9**, PV-Cre mice expressing AAV-DIO-hM4Di-mCherry were fear conditioned (CS1+footshock, 0.5mA) 1hr after injection of CNO or vehicle (VEH). Mice were perfused 90 min later. cfos expression in hM4Di-mCherry positive neurons in the amygdala was assessed. A significant reduction in cfos was observed in PV+ cells in mice injected with CNO compared to VEH injected controls, $F(1,33) = 5.85, P < .001$. $n=15$ for VEH, $n=20$ for CNO.

Surgery

Mice were pre-treated with atropine sulfate (0.1 mg/kg, ip), anesthetized with chloral hydrate (400 mg/kg, ip) and placed in a stereotaxic frame. Skin was retracted and holes drilled in the skull above LA [AP = -1.4 mm, ML = \pm 3.5 mm, V = -5.0 mm from bregma according to (36)]. Bilateral microinjections of HSV vectors (1.5 μ l) were delivered through glass micropipettes over 20 min. Micropipettes were left in place an additional 10 min to ensure diffusion. Unless otherwise specified, mice were trained 3 days following HSV surgery, at a time of maximal transgene expression using this HSV vector system (34). For the optogenetic experiment, mice were similarly microinjected with HSV-NpACY and bilateral optical fibres were implanted slightly above each LA (~0.5 mm)(10, 37, 38). Optical fibres were constructed in-house by attaching a 10 mm piece of 200- μ m, optical fibre (with a 0.37 numerical-aperture, NA) to a 1.25-mm zirconia ferrule (fibre extended 5 mm beyond ferrule). Fibres were attached with epoxy resin into ferrules, cut and polished. Optical fibres were stabilized to the skull with screws and dental cement. Dental cement was painted black to minimize light leakage. After surgery, mice were fitted with plastic caps over implanted optical fibres.

For PV⁺ interneuron modulation experiments, AAV-DIO-hM4Di-mCherry (1.0 μ l) was infused bilaterally into the amygdala using the same approach and co-ordinates described above. After 4 weeks, mice were then microinjected with HSV-NpACY and optical fibres implanted.

Verifying location of vector microinjection and extent of viral infection

At the completion of each experiment, mice were transcardially perfused with 4% paraformaldehyde (PFA) and brains removed. Brains were post-fixed overnight in PFA and coronal brain sections (40 μ m) across entire anterior-posterior extent of LA collected. Every second section was slide-mounted and coverslipped with DAPI-containing mounting medium. The placement and extent of viral infection for each mouse was determined using native immunofluorescence (which did not differ across vectors). For HSV-infusions, only mice determined to show strong bilateral transgene expression limited to the LA (13-20% of LA neurons across 8-10 sections) were included for subsequent data analysis. Consistent with many reports from several labs microinjection of HSV vectors produces robust localized transgene expression with minimal tissue damage around the site of microinjection (34, 39, 40). For mice also infused with AAV-DIO-hM4Di-mCherry, bilateral expression of mCherry in LA/BA was examined and only mice correctly expressing both HSV and AAV transgenes were included in data analysis.

Optogenetic modulation of fear memory: overall design of experiments

Mice used in the optogenetic experiments were trained similarly to those in Fig. 1 except that we increased the intensity of footshocks so as to equalize CS2-freezing levels in mice trained with two Events with short (6h) or long (24h) inter-training intervals. Specifically, Event1 used a 0.45mA footshock, while Event2 used a 0.5mA footshock.

In Figs. 3 and 4 using HSV-NpACY vector, HSV-infected neurons were first excited with blue light stimulation (BL+, 473 nm, 20 Hz, 5 msec pulses, 10 mW peak, 10% duty cycle) for 30 sec before onset of the auditory CS in the training session (Event1). Blue light stimulation did not result in any changes in behavior during the

training session (**fig. S8A**) and blue light alone (without opsin) did not affect freezing during the test session (**fig. S8B**). Red light was delivered in the test session (RL+, 660 nm, 7 mW square pulse) such that mice were presented with the CS twice, one time with RL+ and the other time without RL (counterbalanced).

The effects of increasing excitability before training on memory (Fig. 3B)

Mice were microinjected in the LA with HSV vector (either HSV-NpACY or HSV-GFP) and 3 d later presented with Event1. During Event1 mice were placed in *Context A* and 2 min later, CS1 was paired with footshock (0.5mA)(*see Table 6 below*). For 30s before the onset of CS1 some groups (BL+) were presented with blue light (BL+). Mice in BL- groups did not receive blue light. All mice were tested 24h later. During the test, mice were placed in *Context B* and 2 min later, presented CS1 for 1 min. Two min after this, the CS1 was again presented for 1 min. For half of the mice the red light was presented (RL+) during the first 1-min first presentation of the CS and for the other half Red Light was presented during the second 1-min presentation of the CS. A decrease in freezing during RL+ testing indicates that the infected neurons were allocated to the engram supporting that memory. Data showing no effect of BL+ or opsin expression on training behavior provided in **fig. S8A**.

Table 6: Experimental design for Fig. 3B

<i>Group</i>	<i>Light before training</i>	<i>Training</i>	<i>Light during Test</i>
NpACY BL-	No light	CS+shock(0.5mA)	RL+, RL-
NpACY BL+	BL+ immediately before training	CS+shock(0.5mA)	RL+, RL-
GFP BL+	BL+ immediately before training	CS+shock(0.5mA)	RL+, RL-
NpACY 24hBL+	BL+ 24h before training	CS+shock(0.5mA)	RL+, RL-

Statistical analysis of freezing

Amount of time spent freezing during CS1 or CS2 presentation was compared across groups by Analysis of Variance (ANOVA). Where appropriate, significant effects were further analyzed using Newman-Keuls (NK) or Fisher's Least Square Difference (LSD). For example, data from **Fig. 3B** were analyzed with a *Group* (between factor) X *Red-light-at-testing* (RL+, RL-; within factor) ANOVA which showed a significant interaction $F(3,28) = 17.41, P < .001$. Post-hocs Newman-Keuls performed on the significant interaction showed that freezing levels were only different in NpACY BL+ group when tested under RL+. Therefore, only mice in which a small portion of neurons were excited before training (NpACY BL+) showed decreased freezing when these

Supplementary Figure 8

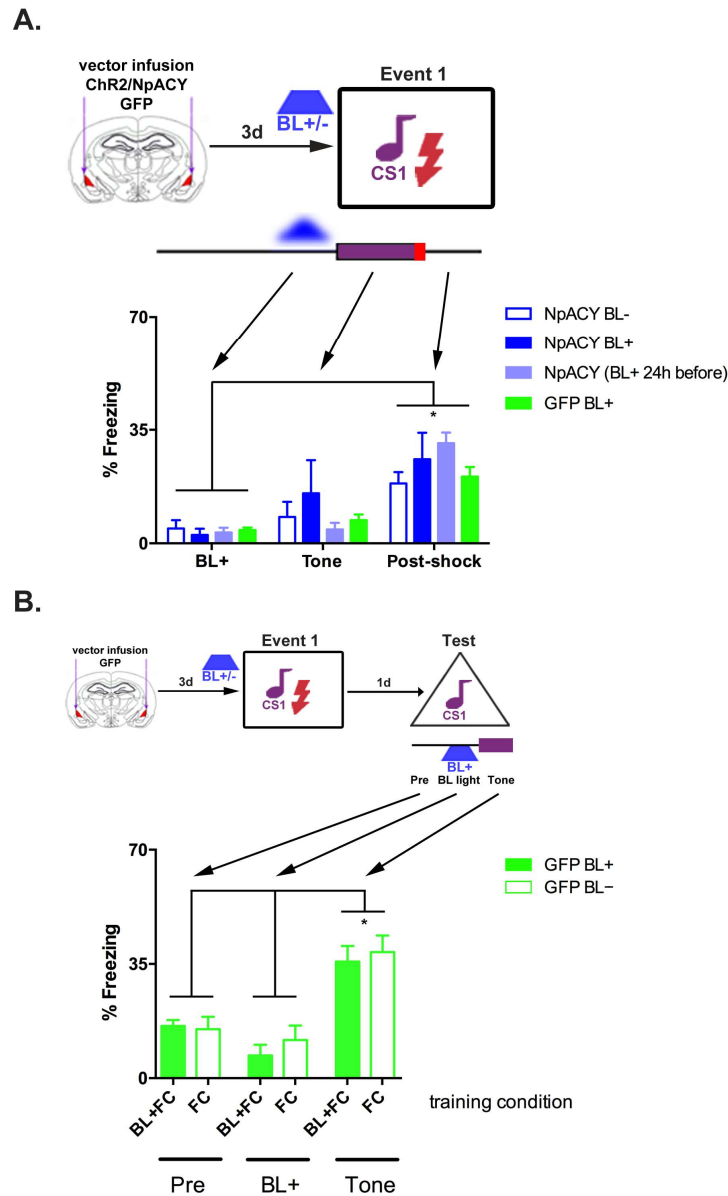


Fig.S8 Blue light activation of ChR2(H134R) in LA does not affect behavior during training

- A. No effects of blue light stimulation were observed on freezing behavior during training [pre tone (during BL+ stimulation), during the tone and post-shock]. A mixed ANOVA (*Group X Training phase* (during blue light, during tone CS, and post-shock) showed no significant interaction $F(6, 56) = 1.26, P > .05$, but a significant overall effect of *Training phase*, with all groups showing greater freezing in the post-shock period (as expected) $F(2, 56) = 36.14, P < .001$. Importantly the absence of main effect or interaction involving *Group*, confirmed that exciting a small portion of LA neurons (NpACy+, BL+) did not enhance memory by changing perception of footshock. $n=8$ for NpACy+, BL-, $n=9$ for NpACy+, BL+, $n=8$ for NpACy+, BL+24h before, $n=7$ for GFP, BL+.
- B. No effect of blue light during test. No difference in freezing between mice (microinjected with HSV-GFP and trained with and without blue light) on testing, either on context exposure alone, blue light alone testing or CS alone testing. A *Group* (BL+ at training, BL- at training) \times *Test* (context only, BL+, CS) ANOVA revealed no significant interaction, $F(2,20) = 0.025, P > .05$, but a significant main effect of *Test*, $F(2,20) = 24.76, P < .001$, in that both groups froze more during CS (as expected). These data confirm that blue light does not become an important cue or occasion setter in this experimental protocol or induce freezing on its own in the test session. $n=6$ /group.

neurons were subsequently silenced by RL during the test. We observed no effect of RL+ in the other control groups (and moreover, these control groups did not differ).

The effects ITI on engram allocation using optogenetics (Fig. 3C)

Mice were microinjected in the LA with HSV-NpACY and 3 d later presented with Event1. During Event1 mice were placed in *Context A* and 2 min later, CS1 was paired with footshock (0.45mA). For 30s before the onset of CS1 all mice were presented with blue light (BL+) to excite and allocate neurons to the engram supporting CS1-shock. Either 6 or 24h later, Event2 occurred. Mice were placed in *Context B* and CS2 was paired with footshock (0.5mA). No light was delivered before or during Event2. 24h later, mice were tested for CS1. As above, during the test, mice were placed in *Context C* and 2 min later, presented CS1 for 1 min. Two min after this, the CS1 was again presented for 1 min. For half of the mice the Red Light was on (RL+) for the first 1-min first presentation of CS1 and for the other half of the mice the Red Light was on for the second 1-min presentation of CS1. 24h later, mice were tested for CS2. A similar procedure took place except that mice were placed in *Context D* and CS2 was presented with or without Red Light. As freezing scores for CS1 did not differ between the 6 and 24h ITI groups, they were combined for an overall score with and without Red light (RL+, RL-).

Co-allocating normally separate engrams by optogenetically exciting neurons (Fig. 3D)

The experiment depicted in Fig. 3D was conducted similar to Fig. 3C except that Event2 occurred 24h following Event1 for all mice. Prior to both Events1 and 2 all mice were given BL+ to allocate the same population of neurons to both engrams. This treatment led to artificial co-allocation of normally separate engrams.

Attempting to separate normally linked engrams by optogenetically inhibiting neurons (Fig. 3E)

The experiment depicted in Fig. 3E was conducted similar to Fig. 3C. Before Event1, all mice were given blue light to allocate neurons to the engram supporting the memory for Event1. Either 6 or 24h later, Event2 occurred. During CS2+footshock pairing, both groups received Red Light (for the duration of CS2 presentation) to inhibit previously allocated neurons. 6h and 24h ITI groups were tested as above. Memory2 was impaired in the 6h ITI group (but not the 24h ITI group), indicating that this technique was unable to separate normally linked memory by simply inhibiting previously “winning” neurons.

Analysis of parvalbumin-expressing interneurons following fear conditioning (Fig. 4A)

WT mice were randomly divided into the following treatment groups; 1) fear conditioning + 3h, 2) fear conditioning + 6h, 3) fear conditioning + 24h, 4) homecage, 5) tone alone + 6h, and 7) immediate shock alone + 6h. Mice were fear conditioned [single CS1+footshock (0.5mA)] or received either the tone or immediate footshock (0.5mA) and returned to homecage and perfused either 3, 6 or 24h later. Homecage mice were taken directly from homecage and not exposed to conditioning chamber, auditory CS or footshock. In this experiment, three control groups were included (homecage, tone alone, immediate shock alone).

Mice were perfused with 4% PFA and vibratome sections (50 μ m) prepared. 8-10 sections per mouse, spanning the LA over the antero-posterior axis were immunostaining for parvalbumin (PV). Sections were processed and imaged in parallel under identical conditions. Sections were incubated with mouse anti-parvalbumin monoclonal antibody (1:1000, Sigma-Aldrich cat#P3088) overnight at 4°C, followed by a 2h incubation at room temperature with an AlexaFluor633-conjugated secondary antibody (1:500, Life Technologies). Sections were counterstained with DAPI as a nuclear stain.

Sections were imaged using identical acquisition parameters. For each image, an optical z-stack was acquired with images $\leq 3 \mu$ m apart. Perisomatic PV innervation of LA neurons was determined using a custom-written macro in ImageJ. To quantify the extent of perisomatic PV innervation, the soma of cells within the LA (50-100 cells per slice, identified by DAPI staining) was outlined and proportion of the perisomatic region (area within a 3 μ m band from the soma) innervated by the neurites of PV interneurons calculated using a manually-calibrated threshold to detect PV fluorescence. In order to exclude non-pyramidal cells, only somas with a feret size between 8-14 μ m were included in analysis based on a frequency distribution of cell size.

Attempting to separate normally linked engrams by optogenetically inhibiting neurons and chemogenetically inhibiting interneurons (Fig. 4B)

The experiment depicted in Fig. 4B was designed to rescue the memory deficits observed in Fig. 3E by silencing PV interneurons before Event2. PV-cre mice were microinjected into the LA/BLA with AAV-DIO-hM4Di-mCherry at least 4 weeks before being microinjected into the LA with HSV-NpACY. In this way, the inhibitory DREADD receptor hM4Di was expressed in PV interneurons and NpACY was expressed in a portion of excitatory principal neurons.

Event1 occurred 3 d after HSV-NpACY microinjection. Before Event1, mice were given blue light (BL+) to allocate HSV-infected neurons to the engram supporting Memory1. Either 6h or 24h later, Event2 occurred. 1h prior to Event2, mice were administered CNO (clozapine N-oxide, 1 mg/kg, ip) or vehicle (VEH). During Event2, mice received Red Light during CS2 presentation to inhibit HSV-infected neurons previously excited and allocated to the engram supporting Event1 memory. Mice were tested for CS1 and CS2 as above.

Picking winners and losers with optogenetics (Fig. 4C)

WT mice were microinjected into the LA with HSV-NpACY. 3d later, Event1 occurred. During Event1 [CS1+footshock (0.45mA) pairing], all mice received Red Light during CS1 presentation (to inhibit infected neurons). 6h later Event2 occurred. 30 s before CS2+footshock (0.5mA) pairing, mice received blue light stimulation to excite infected neurons and allocate them to the engram supporting Memory2. Mice were tested for CS1 and CS2 as above.

Examining CS generalization

The levels of freezing to the 30-sec CS2 during Event2 training (from testing data depicted in Fig. 1B) is presented in **fig. S1D**. An ANOVA conducted on the freezing levels to the 30-sec CS2 revealed a significant effect of *Previous Treatment*, $F(8,142) = 30.49$, $P < .001$. However, there was no difference in freezing between CS1+shock groups (closed orange bars) trained with different ITIs, $F(4,51) = 0.91$, $P > .05$.

Importantly there was no difference between the CS2 freezing levels during this training period between groups that were fear conditioned in Event1 (while only mice trained with short ITI showed enhanced CS2 freezing during the test, Fig. 1B). That is, although mice with a 6h ITI and 24h ITI showed similar levels of freezing to 30 sec-CS2 during training, the 6h ITI groups showed statically higher levels of freezing during the CS2 test (1 min). Therefore, although all previously auditory fear conditioned mice tended to generalize to a limited degree to the second auditory CS, only groups trained with a short ITI subsequently showed enhanced memory for Event2.

Two Events separated by different intervals – reducing generalization (fig. S2)

To more directly control for potential effects of CS generalization, we performed several additional experiments that were designed to minimize the potential generalization of CS2 during Event2 training.

Different sensory modalities of CS (fig. S2A). To eliminate the possibility that generalization to CS2 influenced the present memory-enhancing effects, mice received two fear conditioning Events in which the CSs were of *different sensory modalities*. During Event1 mice received light-shock pairing, while during Event2 (conducted either 6 or 24h later) mice received tone-shock pairing. Consistent with the present data using two auditory CSs, mice trained with a short ITI showed enhanced memory for Event2. A control condition showed that, similar to two auditory stimuli experiments, exposure to a light alone 6h prior to Event2 did not enhance.

Pre-exposure to CSs to reduce generalization between CSs (fig. S2B). Before Event1, mice were pre-exposed to CS1 (5 x 1 min, 1 min intervals) in *Context A*, followed by pre-exposure to CS2 (5 x 1 min, 1 min intervals) in *Context B*. The following day, mice were trained with Event1 followed either 6h or 24h by Event2 (exactly as in Fig. 1B). Mice were tested as in Fig. 1B. During Event2 training, both groups of mice showed similarly low levels of freezing to CS2. However, when tested for Memory2, mice with the short ITI (6h) showed significantly greater freezing to CS2 than mice trained with the longer ITI (24h).

Weak training conditions (fig. S2C). This experiment included 3 groups. Groups 1 and 2 were trained in Event1 and Event2 (no CS pre-exposure) separated by either a 1.5h or 24h ITI (as in **Fig. 1B**). However, the intensity of footshock was weak (0.25mA shock for Event1, 0.3mA shock for Event2). A separate group received CS1 alone presentation during Event1 and were trained (CS2+footshock) for Event2. During Event2 training, previously fear conditioned mice (Groups1 and 2) showed little freezing to CS2, although it was significantly higher than CS1 alone groups, $F(2,45) = 7.63, P < .001$. However, during the subsequent test, mice trained with a 6h ITI froze significantly greater than mice trained with a 24h ITI and mice that received CS1 alone, $F(2,45) = 11.27, P < .001$. Together, these data indicate it is unlikely that generalization between auditory CSs can account for the ITI effects observed in **Fig. 1B**.

Control for time-of-day effects (fig. S1E)

Several studies (41) showed that if trained with a weak training protocol (but importantly, not a stronger training protocol) mice show time-of-day effects on fear conditioning. In the present experiments, Event1 occurred at 9am and Event2 at varying times after Event1 (e.g., for 6h ITI, Event2 occurred at 3pm). Testing was conducted the

next day starting at 9am. Importantly, in the current studies we used fairly robust training that may overcome time-of-day effects.

However, in order to investigate the potential influence of time-of-day on our results more directly, we performed an additional experiment where we trained mice once at 9am or 3pm (CS1+ footshock, 0.45 mA) and tested mice the following day at 9am or 3pm (see Table 7 below).

Table 7: Experimental design for fig. S1F

<i>Training</i>	<i>Test</i>
CS1+shock(0.45mA), 9am	9am
CS1+shock(0.45mA), 3pm	9am
CS1+shock(0.45mA), 9am	3pm
CS1+shock(0.45mA), 3pm	3pm

pCREB and ICER expression time-course in neuronal cultures (fig. S4)

Primary cortical neuronal cell cultures were prepared from WT mice (E18-19) as previous (11). After 10 d in culture, neurons were given stimulation pulse [30 μ M forskolin (FSK) and 55mM KCl applied to medium] or left non-treated (NT). Neurons were collected at different times after stimulation and homogenized in cell lysis buffer (50 mM Tris, 0.25 M sucrose, 25 mM KCl, 5 mM MgCl₂ with protease and phosphatase inhibitors), sonicated for 5 min and resuspended in buffer (100 mM Tris.Cl, pH 6.8, 200 mM DTT, 4% SDS, 20% glycerol and 0.2% bromophenol blue).

Homogenates were separated by SDS-polyacrylamide gel electrophoresis and electroblotted onto PVDF transfer membranes. Membranes were blocked for 1 h in 10% skimmed milk in Tris-buffered saline (TBS) and incubated overnight at 4°C with the following primary antibodies in 1% skimmed milk in TBS: mouse anti-CREB (1:1000, Millipore), rabbit anti-pCREB S133 (1:1000, Cell Signaling), rabbit anti-ICER/CREM (1:1000, Pierce Antibodies) and rabbit anti-glyceraldehyde-3-phosphate (GAPDH) (1:5000, Cell Signaling). After overnight incubation, membranes were washed with TBS, 0.1% Tween-20 for 10 min and incubated for 2 h at room temperature with an HRP-conjugated species-specific secondary antibody. Bands were visualized by exposure of membranes to film following treatment with Western Blotting Detection Reagents. The optical intensity of bands associated with ICER and CREB was measured relative to their respective GAPDH bands. pCREB was measured relative to respective CREB bands on the same blot using Image J.

Electrophysiological validation of NpACY construct (fig. S5)

Primary cultured hippocampal neurons and recording experiments were performed as previously described (18, 42).

Cell specificity of HSV infection (fig. S6)

We used HSV to manipulate excitability in excitatory principal neurons in the LA. We previously showed that HSV viral vectors microinjected into the LA overwhelmingly infected excitatory neurons (10). To verify this, we microinjected mice with HSV-GFP into the LA, and 4 d later, perfused mice transcardially with 4% paraformaldehyde (PFA). Brains were sliced coronally (50 μ m) and incubated with GFP (to visualize infected cells; rabbit; 1:1000, Millipore), GFAP (Glial Fibrillary Acidic Protein, to label astrocytes; mouse; 1:1000, Cell Signaling), α -CaMKII (alpha Ca^{2+} /calmodulin-dependent protein kinase II; to label excitatory principal neurons, mouse; 1:1000, C265, Millipore), GAD67 (Glutamate decarboxylase 67, to label inhibitory neurons, mouse; 1:500, 1G10.2, Millipore) or PV (parvalbumin, to label parvalbumin positive inhibitory neurons, mouse; 1:1000, P3088, Sigma-Aldrich) in blocking solution for 24 h at 4°C. Slices were then incubated with secondary goat anti-rabbit ALEXA 568 (1141875; 1:500, Invitrogen, Eugene, Oregon) and goat anti-rabbit ALEXA 488 (1141875; 1:500, Invitrogen, Eugene, Oregon) antibodies for 2 h at room temperature. Slices were washed with PBS 0.1M, counterstained with DAPI (4',6-diamidino-2-phenylindol) and mounted on gelatin-coated slides. Images were acquired with a Zeiss LSM710 confocal microscope and were analyzed using ImageJ software.

***In vivo* validation of constructs (cfos expression) (fig. S7)**

To validate the optogenetic tools used in the present experiments, molecular markers of neuronal activity (*cfos*) *ex vivo* were used (fig. S7A). Mice were injected with NpACY vector as in the behavioral experiments and LA *cfos* was analyzed 90 min following:

1. blue light before fear conditioning (CS1+0.5mA shock, BL+, FC group).
2. no blue light before fear conditioning (BL-, FC group).
3. red light during fear conditioning (RL+, FC group).
4. blue light only, no fear conditioning (BL+, no FC group).

Immunostaining for *cfos* was performed as previously described (10) on 12-16 sections per mouse, spanning the antero-posterior axis of the LA. Sections were processed and imaged in parallel under identical conditions. Briefly, sections were incubated with rabbit anti-*fos* polyclonal antibody (sc-52, 1:500, Santa Cruz) overnight at 4°C, followed by a 2 h incubation at room temperature with an Alexa633-conjugated goat anti-rabbit secondary antibody (A21070; 1:1 000, Life Technologies). Sections were counterstained with DAPI to visualize nuclei. Images were acquired (Zeiss LSM710 confocal microscope) and analyzed (ImageJ software).

To ensure heat generated by blue light itself did not contribute to the observed effect (43), we shone blue light in the LA of mice infused with HSV-GFP and perfused mice 90 min later for *cfos* analysis. Our laser was set to produce a 20Hz square wave with 10mW peak power. For 10% duty cycle, each pulse was 5 msec in width (with a 45 msec gap between pulses), giving an average power of 1mW. For 50% duty cycle, each pulse was 25 msec in width (with 25 msec in between pulses). Blue light stimulation was for 30 sec, as in the behavioral experiments. Expression of *cfos* in each condition (10%

duty cycle, 50% duty cycle) was compared to mice that were fear conditioned but did not receive light stimulation (**fig. S7B**).

To validate the DREADD construct (hM4Di) used in Fig. 4, PV-Cre mice expressing AAV-DIO-hM4Di-mCherry were fear conditioned (CS1+footshock, 0.5mA) 1hr after injection of CNO (1mg/kg, i.p) or vehicle. Mice were perfused 90 min later and assessed for cfos expression in hM4Di-mCherry positive neurons of the amygdala (**fig. S7C**).

Effects of blue light on behavior during fear testing (fig. S8B)

To directly assess whether the blue light acted as a “cue” or occasion setter for the CS-US pairing or somehow non-specifically increased freezing during the memory test, we performed an experiment in which mice were microinjected with HSV-GFP (no opsin) vector. Mice were divided into 2 groups. One group (BL+) received blue light (20Hz for 30 sec, the same parameters as in experimental groups) before CS-US (0.5mA footshock) pairing and the other group did not receive light before CS-US pairing (BL-). All mice were tested 24 h later. During the test, mice were placed in a novel context and given no stimulation for 2 min, then blue light stimulation for one minute (BL+ on graph), followed by another habituation period (2 min) and presentation of the CS for 1 min. Freezing was assessed during these test periods.

Supplementary Figure 9

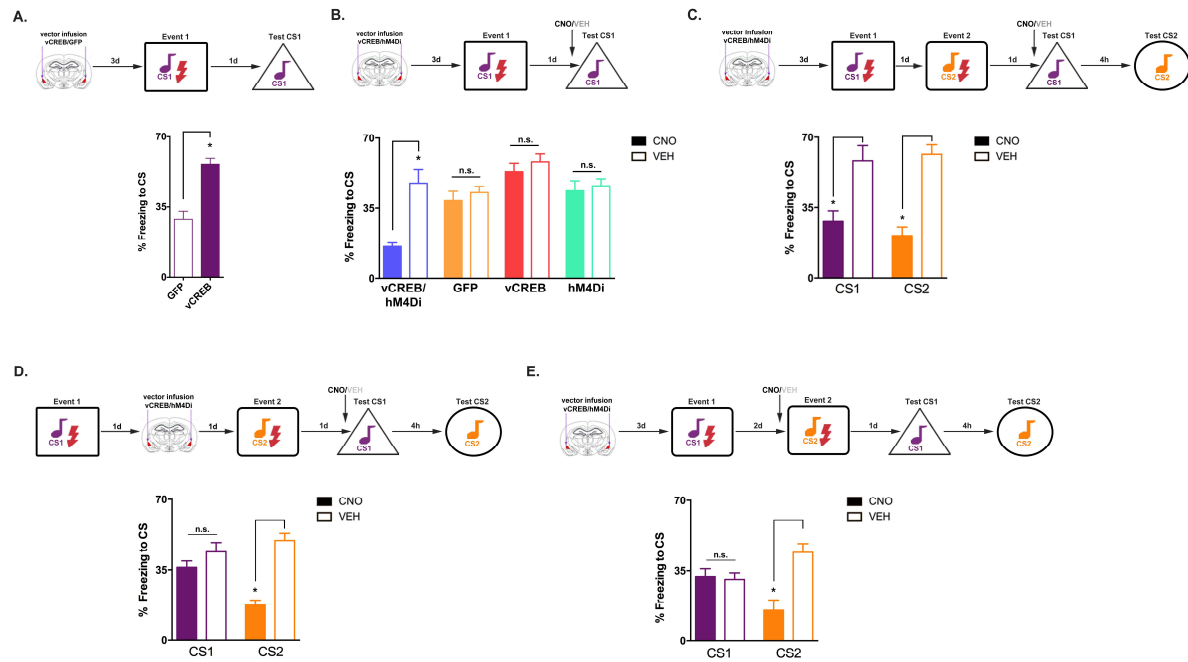


Fig. S9. Memory allocation and co-allocation using CREB to excite neurons and DREADDs to inhibit their activity.

- Increasing CREB in a small population of LA principal neurons enhances fear memory formation, $F(1,15) = 26.78$, $P < .001$, $n = 8$ per group.
- Neuron expressing vCREB are preferentially allocated to the engram supporting a fear memory. Mice microinjected HSV that co-expressed vCREB and inhibitory DREADD, hM4Di. Control groups received HSV vector expressing either vCREB alone, hM4Di alone or GFP. Mice were given auditory fear conditioning and tested 1 d later. Before testing, mice received either CNO, to silence neurons expressing hM4Di, or vehicle (VEH). *Vector* (vCREB/hM4Di, GFP, vCREB, hM4Di) X *Drug* (CNO, VEH) ANOVA showed a significant interaction, $F(3,69) = 6.28$, $P < .001$. CNO or VEH injections had no effect on mice expressing GFP, vCREB or hM4Di alone, but decreased memory expression in mice expressing vCREB and hM4Di in the same neurons, by post-hoc. $n=8-12$ for each group. Therefore, silencing neurons allocated to the engram (using vCREB to allocate neurons and hM4Di to subsequently silence these neurons during the test) impairs memory expression. This result served as proof-of-principle for (C) and (D) of this figure.
- Linking normally separated memories (24h ITI) by virally overexpressing CREB (vCREB) to excite the same neurons during Event1 and Event2. Neurons expressing vCREB were preferentially allocated to both engrams, as silencing infected neurons (CNO) was sufficient to impair expression of both memories. *Group* (CREB-hM4Di+CNO before test, CREB-hM4Di+VEH before test) X *CS-freezing* (CS1, CS2) ANOVA revealed no significant interaction, but significant main effect of *Group*, $F(1,15) = 23.69$, $P < .001$. $n=9$ for VEH, $n=8$ for CNO.
- Silencing a population of LA neurons does not non-specifically impair expression of all conditioned fear memories. Mice microinjected with HSV-vCREB/hM4Di after Event1 (infected neurons were unlikely to be part of engram supporting memory for Event1). 24h after microinjection, mice trained on Event2 (HSV-infected neurons allocated to the engram supporting Event2 memory). Mice were tested after CNO administration to silence infected neurons. Memory for Event1 was intact, but memory for Event2 was disrupted, *Group* (CREB-hM4Di+CNO before test, CREB-hM4Di+VEH before test) X *CS-freezing* (CS1, CS2) ANOVA revealed a significant interaction, $F(1,14) = 32.39$, $P < .001$. Post-hoc tests revealed that freezing levels to CS1 were not different between CNO and VEH conditions, whereas CS2 freezing was decreased by CNO. $n=5$ for VEH, $n=11$ for CNO.
- Attempting to separate normally linked memories using vCREB to excite neurons and hM4Di to inhibit infected neurons. Mice microinjected with HSV-vCREB/hM4Di before Event1 and Event2 (separated by 48h ITI). Neurons expressing vCREB co-allocated to engrams supporting both Event1 and Event2 (vCREB expression continued for several days). To separate these normally linked memories, we silenced infected neurons (CNO) before Event2. Mice were tested for CS1 and CS2 drug-free. Both groups showed intact memory for CS1. However, mice treated with CNO before Event2 showed impaired Event2 memory. *Group* (CREB-hM4Di+CNO before Event2, CREB-hM4Di+VEH before Event2) X *CS-freezing* (CS1, CS2) ANOVA revealed a significant interaction, $F(1,10) = 22.06$, $P < .001$. $n=7$ for VEH, $n=5$ for CNO. These findings are in agreement with the findings of Fig. 3E, 4B showing that inhibiting neurons allocated to Event1 during training for Event2 impaired the acquisition of memory for Event2 if these allocated neurons continued to be more excitable than their neighbors (as is the case with vCREB).

References and Notes

1. S. A. Josselyn, S. Köhler, P. W. Frankland, Finding the engram. *Nat. Rev. Neurosci.* **16**, 521–534 (2015). [doi:10.1038/nrn4000](https://doi.org/10.1038/nrn4000) [Medline](#)
2. S. Tonegawa, X. Liu, S. Ramirez, R. Redondo, Memory engram cells have come of age. *Neuron* **87**, 918–931 (2015). [doi:10.1016/j.neuron.2015.08.002](https://doi.org/10.1016/j.neuron.2015.08.002) [Medline](#)
3. J. E. LeDoux, Emotion circuits in the brain. *Annu. Rev. Neurosci.* **23**, 155–184 (2000). [doi:10.1146/annurev.neuro.23.1.155](https://doi.org/10.1146/annurev.neuro.23.1.155) [Medline](#)
4. S. Maren, The amygdala, synaptic plasticity, and fear memory. *Ann. N. Y. Acad. Sci.* **985**, 106–113 (2003). [doi:10.1111/j.1749-6632.2003.tb07075.x](https://doi.org/10.1111/j.1749-6632.2003.tb07075.x) [Medline](#)
5. S. Duvarci, D. Pare, Amygdala microcircuits controlling learned fear. *Neuron* **82**, 966–980 (2014). [doi:10.1016/j.neuron.2014.04.042](https://doi.org/10.1016/j.neuron.2014.04.042) [Medline](#)
6. D. Kim, D. Paré, S. S. Nair, Assignment of model amygdala neurons to the fear memory trace depends on competitive synaptic interactions. *J. Neurosci.* **33**, 14354–14358 (2013). [doi:10.1523/JNEUROSCI.2430-13.2013](https://doi.org/10.1523/JNEUROSCI.2430-13.2013) [Medline](#)
7. J. H. Han, S. A. Kushner, A. P. Yiu, C. J. Cole, A. Matynia, R. A. Brown, R. L. Neve, J. F. Guzowski, A. J. Silva, S. A. Josselyn, Neuronal competition and selection during memory formation. *Science* **316**, 457–460 (2007). [doi:10.1126/science.1139438](https://doi.org/10.1126/science.1139438) [Medline](#)
8. J. H. Han, S. A. Kushner, A. P. Yiu, H.-L. Hsiang, T. Buch, A. Waisman, B. Bontempi, R. L. Neve, P. W. Frankland, S. A. Josselyn, Selective erasure of a fear memory. *Science* **323**, 1492–1496 (2009). [doi:10.1126/science.1164139](https://doi.org/10.1126/science.1164139) [Medline](#)
9. Y. Zhou, J. Won, M. G. Karlsson, M. Zhou, T. Rogerson, J. Balaji, R. Neve, P. Poirazi, A. J. Silva, CREB regulates excitability and the allocation of memory to subsets of neurons in the amygdala. *Nat. Neurosci.* **12**, 1438–1443 (2009). [doi:10.1038/nn.2405](https://doi.org/10.1038/nn.2405) [Medline](#)
10. A. P. Yiu, V. Mercaldo, C. Yan, B. Richards, A. J. Rashid, H.-L. L. Hsiang, J. Pressey, V. Mahadevan, M. M. Tran, S. A. Kushner, M. A. Woodin, P. W. Frankland, S. A. Josselyn, Neurons are recruited to a memory trace based on relative neuronal excitability immediately before training. *Neuron* **83**, 722–735 (2014). [doi:10.1016/j.neuron.2014.07.017](https://doi.org/10.1016/j.neuron.2014.07.017) [Medline](#)
11. L. A. Gouty-Colomer, B. Hosseini, I. M. Marcelo, J. Schreiber, D. E. Slump, S. Yamaguchi, A. R. Houweling, D. Jaarsma, Y. Elgersma, S. A. Kushner, Arc expression identifies the lateral amygdala fear memory trace. *Mol. Psychiatry* **21**, 364–375 (2016). [doi:10.1038/mp.2015.18](https://doi.org/10.1038/mp.2015.18) [Medline](#)
12. J. F. Guzowski, Insights into immediate-early gene function in hippocampal memory consolidation using antisense oligonucleotide and fluorescent imaging approaches. *Hippocampus* **12**, 86–104 (2002). [doi:10.1002/hipo.10010](https://doi.org/10.1002/hipo.10010) [Medline](#)
13. M. M. Oh, A. G. Kuo, W. W. Wu, E. A. Sametsky, J. F. Disterhoft, Watermaze learning enhances excitability of CA1 pyramidal neurons. *J. Neurophysiol.* **90**, 2171–2179 (2003). [doi:10.1152/jn.01177.2002](https://doi.org/10.1152/jn.01177.2002) [Medline](#)

14. L. T. Thompson, J. R. Moyer Jr., J. F. Disterhoft, Transient changes in excitability of rabbit CA3 neurons with a time course appropriate to support memory consolidation. *J. Neurophysiol.* **76**, 1836–1849 (1996). [Medline](#)
15. L. Monaco, N. S. Foulkes, P. Sassone-Corsi, Pituitary follicle-stimulating hormone (FSH) induces CREM gene expression in Sertoli cells: Involvement in long-term desensitization of the FSH receptor. *Proc. Natl. Acad. Sci. U.S.A.* **92**, 10673–10677 (1995). [doi:10.1073/pnas.92.23.10673](#) [Medline](#)
16. A. J. Silva, Y. Zhou, T. Rogerson, J. Shobe, J. Balaji, Molecular and cellular approaches to memory allocation in neural circuits. *Science* **326**, 391–395 (2009). [doi:10.1126/science.1174519](#) [Medline](#)
17. Y. Mei, F. Zhang, Molecular tools and approaches for optogenetics. *Biol. Psychiatry* **71**, 1033–1038 (2012). [doi:10.1016/j.biopsych.2012.02.019](#) [Medline](#)
18. V. Gradinaru, F. Zhang, C. Ramakrishnan, J. Mattis, R. Prakash, I. Diester, I. Goshen, K. R. Thompson, K. Deisseroth, Molecular and cellular approaches for diversifying and extending optogenetics. *Cell* **141**, 154–165 (2010). [doi:10.1016/j.cell.2010.02.037](#) [Medline](#)
19. B. N. Armbruster, X. Li, M. H. Pausch, S. Herlitze, B. L. Roth, Evolving the lock to fit the key to create a family of G protein-coupled receptors potently activated by an inert ligand. *Proc. Natl. Acad. Sci. U.S.A.* **104**, 5163–5168 (2007). [doi:10.1073/pnas.0700293104](#) [Medline](#)
20. P. A. Shoemaker, Neuronal networks with NMDARs and lateral inhibition implement winner-takes-all. *Front. Comput. Neurosci.* **9**, 12 (2015). [doi:10.3389/fncom.2015.00012](#) [Medline](#)
21. P. Sah, E. S. Faber, M. Lopez De Armentia, J. Power, The amygdaloid complex: Anatomy and physiology. *Physiol. Rev.* **83**, 803–834 (2003). [doi:10.1152/physrev.00002.2003](#) [Medline](#)
22. S. B. Wolff, J. Gründemann, P. Tovote, S. Krabbe, G. A. Jacobson, C. Müller, C. Herry, I. Ehrlich, R. W. Friedrich, J. J. Letzkus, A. Lüthi, Amygdala interneuron subtypes control fear learning through disinhibition. *Nature* **509**, 453–458 (2014). [doi:10.1038/nature13258](#) [Medline](#)
23. A. R. Woodruff, P. Sah, Networks of parvalbumin-positive interneurons in the basolateral amygdala. *J. Neurosci.* **27**, 553–563 (2007). [doi:10.1523/JNEUROSCI.3686-06.2007](#) [Medline](#)
24. S. Trouche, J. M. Sasaki, T. Tu, L. G. Reijmers, Fear extinction causes target-specific remodeling of perisomatic inhibitory synapses. *Neuron* **80**, 1054–1065 (2013). [doi:10.1016/j.neuron.2013.07.047](#) [Medline](#)
25. D. J. Cai, D. Aharoni, T. Shuman, J. Shobe, J. Biane, W. Song, B. Wei, M. Veshkini, M. La-Vu, J. Lou, S. E. Flores, I. Kim, Y. Sano, M. Zhou, K. Baumgaertel, A. Lavi, M. Kamata, M. Tuszyński, M. Mayford, P. Golshani, A. J. Silva, A shared neural ensemble links distinct contextual memories encoded close in time. *Nature* **534**, 115–118 (2016). [Medline](#) [doi:10.1038/nature17955](#)

26. S. Hippenmeyer, E. Vrieseling, M. Sigrist, T. Portmann, C. Laengle, D. R. Ladle, S. Arber, A developmental switch in the response of DRG neurons to ETS transcription factor signaling. *PLoS Biol.* **3**, e159 (2005). [doi:10.1371/journal.pbio.0030159](https://doi.org/10.1371/journal.pbio.0030159) [Medline](#)
27. M. S. Fanselow, Factors governing one trial contextual conditioning. *Anim. Learn. Behav.* **18**, 264–270 (1990). [doi:10.3758/BF03205285](https://doi.org/10.3758/BF03205285)
28. P. W. Frankland, S. A. Josselyn, S. G. Anagnostaras, J. H. Kogan, E. Takahashi, A. J. Silva, Consolidation of CS and US representations in associative fear conditioning. *Hippocampus* **14**, 557–569 (2004). [doi:10.1002/hipo.10208](https://doi.org/10.1002/hipo.10208) [Medline](#)
29. B. J. Wiltgen, M. J. Sanders, N. S. Behne, M. S. Fanselow, Sex differences, context preexposure, and the immediate shock deficit in Pavlovian context conditioning with mice. *Behav. Neurosci.* **115**, 26–32 (2001). [doi:10.1037/0735-7044.115.1.26](https://doi.org/10.1037/0735-7044.115.1.26) [Medline](#)
30. D. Bottai, J. F. Guzowski, M. K. Schwarz, S. H. Kang, B. Xiao, A. Lanahan, P. F. Worley, P. H. Seeburg, Synaptic activity-induced conversion of intronic to exonic sequence in Homer 1 immediate early gene expression. *J. Neurosci.* **22**, 167–175 (2002). [Medline](#)
31. J. H. Han, A. P. Yiu, C. J. Cole, H.-L. Hsiang, R. L. Neve, S. A. Josselyn, Increasing CREB in the auditory thalamus enhances memory and generalization of auditory conditioned fear. *Learn. Mem.* **15**, 443–453 (2008). [doi:10.1101/lm.993608](https://doi.org/10.1101/lm.993608) [Medline](#)
32. W. A. Carlezon Jr., E. J. Nestler, R. L. Neve, Herpes simplex virus-mediated gene transfer as a tool for neuropsychiatric research. *Crit. Rev. Neurobiol.* **14**, 47–67 (2000). [doi:10.1615/CritRevNeurobiol.v14.i1.30](https://doi.org/10.1615/CritRevNeurobiol.v14.i1.30) [Medline](#)
33. C. J. Cole, V. Mercaldo, L. Restivo, A. P. Yiu, M. J. Sekeres, J.-H. Han, G. Vetere, T. Pekar, P. J. Ross, R. L. Neve, P. W. Frankland, S. A. Josselyn, MEF2 negatively regulates learning-induced structural plasticity and memory formation. *Nat. Neurosci.* **15**, 1255–1264 (2012). [doi:10.1038/nn.3189](https://doi.org/10.1038/nn.3189) [Medline](#)
34. M. Barrot, J. D. A. Olivier, L. I. Perrotti, R. J. DiLeone, O. Berton, A. J. Eisch, S. Impey, D. R. Storm, R. L. Neve, J. C. Yin, V. Zachariou, E. J. Nestler, CREB activity in the nucleus accumbens shell controls gating of behavioral responses to emotional stimuli. *Proc. Natl. Acad. Sci. U.S.A.* **99**, 11435–11440 (2002). [doi:10.1073/pnas.172091899](https://doi.org/10.1073/pnas.172091899) [Medline](#)
35. M. J. Krashes, S. Koda, C. Ye, S. C. Rogan, A. C. Adams, D. S. Cusher, E. Maratos-Flier, B. L. Roth, B. B. Lowell, Rapid, reversible activation of AgRP neurons drives feeding behavior in mice. *J. Clin. Invest.* **121**, 1424–1428 (2011). [doi:10.1172/JCI46229](https://doi.org/10.1172/JCI46229) [Medline](#)
36. G. Paxinos, K. B. J. Franklin, *The Mouse Brain in Stereotaxic Coordinates*, 2nd Edn., (Academic Press, San Diego, 2001).
37. D. R. Sparta, A. M. Stamatakis, J. L. Phillips, N. Hovelsø, R. van Zessen, G. D. Stuber, Construction of implantable optical fibers for long-term optogenetic manipulation of neural circuits. *Nat. Protoc.* **7**, 12–23 (2011). [doi:10.1038/nprot.2011.413](https://doi.org/10.1038/nprot.2011.413) [Medline](#)
38. G. D. Stuber, D. R. Sparta, A. M. Stamatakis, W. A. van Leeuwen, J. E. Hardjoprajitno, S. Cho, K. M. Tye, K. A. Kempadoo, F. Zhang, K. Deisseroth, A. Bonci, Excitatory transmission from the amygdala to nucleus accumbens facilitates reward seeking. *Nature* **475**, 377–380 (2011). [doi:10.1038/nature10194](https://doi.org/10.1038/nature10194) [Medline](#)

39. W. A. Carlezon Jr., R. L. Neve, Viral-mediated gene transfer to study the behavioral correlates of CREB function in the nucleus accumbens of rats. *Methods Mol. Med.* **79**, 331–350 (2003). [Medline](#)
40. J. W. Koo, M. S. Mazei-Robison, Q. LaPlant, G. Egervari, K. M. Braunscheidel, D. N. Adank, D. Ferguson, J. Feng, H. Sun, K. N. Scobie, D. M. Domez-Werno, E. Ribeiro, C. J. Peña, D. Walker, R. C. Bagot, M. E. Cahill, S. A. Anderson, B. Labonté, G. E. Hodes, H. Browne, B. Chadwick, A. J. Robison, V. F. Vialou, C. Dias, Z. Lorsch, E. Mouzon, M. K. Lobo, D. M. Dietz, S. J. Russo, R. L. Neve, Y. L. Hurd, E. J. Nestler, Epigenetic basis of opiate suppression of Bdnf gene expression in the ventral tegmental area. *Nat. Neurosci.* **18**, 415–422 (2015). [Medline](#)
41. D. Chaudhury, C. S. Colwell, Circadian modulation of learning and memory in fear-conditioned mice. *Behav. Brain Res.* **133**, 95–108 (2002).[doi:10.1016/S0166-4328\(01\)00471-5](https://doi.org/10.1016/S0166-4328(01)00471-5) [Medline](#)
42. A. Berndt, S. Y. Lee, J. Wietek, C. Ramakrishnan, E. E. Steinberg, A. J. Rashid, H. Kim, S. Park, A. Santoro, P. W. Frankland, S. M. Iyer, S. Pak, S. Ährlund-Richter, S. L. Delp, R. C. Malenka, S. A. Josselyn, M. Carlén, P. Hegemann, K. Deisseroth, Structural foundations of optogenetics: Determinants of channelrhodopsin ion selectivity. *Proc. Natl. Acad. Sci. U.S.A.* **113**, 822–829 (2016).[doi:10.1073/pnas.1523341113](https://doi.org/10.1073/pnas.1523341113) [Medline](#)
43. J. M. Stujenske, T. Spellman, J. A. Gordon, Modeling the spatiotemporal dynamics of light and heat propagation for in vivo optogenetics. *Cell Reports* **12**, 525–534 (2015).[doi:10.1016/j.celrep.2015.06.036](https://doi.org/10.1016/j.celrep.2015.06.036) [Medline](#)